Atmospheric Environment 45 (2011) 7184–7191

Contents lists available at SciVerse ScienceDirect

Atmospheric Environment

journal homepage: www.elsevier.com/locate/atmosenv

Roadside and rooftop measurements of polycyclic aromatic hydrocarbons in $PM_{2.5}$ in urban Guangzhou: Evaluation of vehicular and regional combustion source contributions

Bo Gao[a], Jian-Zhen Yu[b,c], Shu-Xian Li[d], Xiang Ding[a,e], Quan-Fu He[a], Xin-Ming Wang[a,*]

[a] State Key Laboratory of Organic Geochemistry, Guangzhou Institute of Geochemistry, Chinese Academy of Sciences, Guangzhou 510640, China
[b] Department of Chemistry, Hong Kong University of Science and Technology, Clear Water Bay, Kowloon, Hong Kong, China
[c] Division of Environment, Hong Kong University of Science and Technology, Clear Water Bay, Kowloon, Hong Kong, China
[d] School of Chemistry and Medicine, Jiamusi University, Jiamusi 154007, China
[e] Pearl River Delta Research Center of Environmental Pollution and Control, Chinese Academy of Sciences, Guangzhou 510640, China

ARTICLE INFO

Article history:
Received 10 June 2011
Received in revised form
25 August 2011
Accepted 1 September 2011

Keywords:
PAHs
Vehicular emissions
Regional
Elemental carbon
Guangzhou

ABSTRACT

Concurrent sampling of $PM_{2.5}$ aerosol at a roadside of heavy traffic (1.2 m above ground) and on a nearby rooftop (50 m above ground) was conducted at a same location in urban Guangzhou in September, October 2006 and January 2007. The samples were analyzed for eighteen polycyclic aromatic hydrocarbons (PAHs), together with major aerosol constituents and certain organic tracers for vehicular emissions (hopanes) and biomass burning (levoglucosan). Elemental carbon (EC) and hopanes were observed to be lower by 21–38% and 28–84%, respectively, at the rooftop than the roadside, confirming vehicular emissions as a significant local PM source. On the other hand, sulfate showed little vertical gradient, consistent with its secondary origin and its regional characteristics. The roadside-rooftop sample pairs have provided an opportunity in evaluating relative contributions of vehicular emissions and regional sources to ambient PAHs in this urban location. Concentrations of the total PAHs were ~43% lower at rooftop in the September 2006 samples while they were at similar levels between rooftop and roadside in the October 2006 and January 2007 samples. Sources of PAHs were investigated through comparing ambient data of PAH isomer pairs and PAH/EC ratios with relevant source profiles including those of Guangzhou roadway tunnel emissions, rice straw/sugarcane leave combustion, and industrial coal combustion. The 4-ring PAHs such as pyrene and fluoranthene had a shift in their dominating source from vehicular emissions in September and October to regional combustion source in January. A few major 5- and 6-ring PAHs such as benzo[ghi]perylene and indeno[1,2,3-cd]pyrene were likely heavily influenced by regional biomass burning emissions in all three sampling months.

Benzo(a)pyrene-equivalent carcinogenic potency (BaP_{eq}) was calculated to evaluate the cancer risk of carcinogenic PAHs on the public. BaP_{eq} levels in $PM_{2.5}$ were significantly higher at the roadside than those at the rooftop in September; however, levels of BaP_{eq} at the rooftop were drastically elevated and became comparable to those at the roadside in October and January due to regional sources dominating the carcinogenic PAHs. This suggests that it is important to control regional combustion sources to reduce air pollution-related health risk in urban Guangzhou.

1. Introduction

Polycyclic aromatic hydrocarbons (PAHs) are primarily emitted by incomplete combustion of fossil fuels and biomass (Bi et al., 2003; Ding et al., 2007; Li et al., 2006; Mai et al., 2003). They have attracted great concern because several of them are known human carcinogens and can be transformed to more toxic daughter compounds in the ambient atmosphere (Marr et al., 2006). Sixteen PAHs are on the list of USEPA's 188 hazardous air pollutants. PAHs with 4–6 aromatic rings have a significant presence in $PM_{2.5}$ (particles with aerodynamic diameter less than 2.5 μm) (Poster et al., 1995). The fine particles can deposit in the lungs and exert their carcinogenicity over long exposure periods.

Guangzhou, with an area of 7434 km^2, is the economic and cultural center of the Pearl River Delta (PRD). During the past decade, its population has increased from 6.9 million in 2000 to

* Corresponding author. Tel.: +8620 85290180; fax: +8620 85290706.
E-mail address: wangxm@gig.ac.cn (X.-M. Wang).

1352-2310/$ – see front matter © 2011 Elsevier Ltd. All rights reserved.
doi:10.1016/j.atmosenv.2011.09.005

over 14 million in 2010. In 1991, there were 0.58 million vehicles in Guangzhou (Bi et al., 2003). By 2007, the number increased to 1.7 million (Wang et al., 2008). The economic development and increase in vehicle numbers have exacted a toll on the air quality. A 52-year record showed that the haze day occurrences in Guangzhou rapidly increased between 1972 and 1980 and remained at ~150 days per year from 1980 to 2006 (Deng et al., 2008). In an extreme case, the instantaneous visibility was less than 200 m in Guangzhou (Wu et al., 2005).

In a number of past studies, PAH levels in Guangzhou were measured and their sources were examined. Bi et al. (2003) identified vehicle emissions as the major source of PAHs in the Li Wan district on the basis of molecular diagnostic ratios. Li et al. (2006) postulated that partition effect was not important in an even temperature area such as Guangzhou and used principal component analysis in combination with multiple linear regression to identify the sources of gas phase and particulate phase. They concluded that vehicle exhaust and industrial coal combustion were major sources of particulate PAHs in Guangzhou. Guangzhou is a subtropical city absent of coal combustion for space heating. Coal combustion is mainly used for power generation. Coal combustion may not be a seasonally dependent source for PAHs and was estimated to contribute around 20–30% of PAHs in the air of Guangzhou (Li et al., 2006). However, it is also recognized that extensive burning of crop residues exists in rural areas in the PRD (Lin et al., 2010). The contribution of biomass burning cannot be ignored. Xu et al. (2006) estimated on the basis of fuel consumption that contribution to total PAHs from biomass burning was up to 83% in Guangdong province. Cooking is another potential source of PAHs (Hu et al., 2007). In China's highly developed regions like urban Guangzhou, however, LPG/LNG (called "pipe-gas") is the dominant fuel for cooking. The contribution of cooking emissions to ambient PAHs is therefore negligible compared to other sources.

PAHs are vulnerable to photochemical oxidation in the atmosphere (Ding et al., 2007; van Drooge and Ballesta, 2009). For this reason, the reliability of the diagnostic ratio method is questionable because oxidization alters the chemical composition of PAHs. Reduced ratio of the relative reactively PAHs to the relatively stable ones would certainly bias estimation of source contributions. In this work, we adopt the ratio–ratio plot method, which was first proposed by Robison et al. (Robinson et al., 2006), to identify the major contributing sources. This method allows illustration of ambient data, mixing of emissions from different sources, and possible photochemical aging in one plot.

In this work, we utilize concurrently collected roadside and rooftop samples at a Guangzhou urban site to evaluate the relative importance of vehicular emissions and regional combustion sources to ambient PAHs. The roadside samples were significantly influenced by local vehicular emissions due to its proximity to traffic. The sample collection periods in this study coincided with a high visibility period (visibility: 18–36 km) and two haze periods (visibility: <10 km). We also aim to characterize the differences in PAH abundances and their carcinogenic potency between the haze and non-haze periods.

2. Materials and method

2.1. Sampling

$PM_{2.5}$ samples were collected simultaneously at a roadside and a rooftop location in urban Guangzhou (Fig. S1). The roadside sampling location was on the sidewalk of a main traffic road (Dongfengdong Road), approximately 0.5 m from the curbside and 1.2 m above ground. Traffic flow reached approximately 6000 motor vehicles (cars, buses and trucks) per hour in rush hours. For this site, about 15% of the motor vehicles were diesel-fueled buses and trucks and others were gasoline-fueled cars. The rooftop site was located on the rooftop of the 15-storey central building in the campus of Guangdong University of Technology (GUT, 23° 07.840′N, 113° 18.020′E), approximately 50 m above ground. The GUT campus is situated between two main roads of heavy traffic (Dongfengdong Road and Huanshidong Road), and the building is approximately 200 m away from the two main roads. The roadside represents a microenvironment of maximal exposure to $PM_{2.5}$ from traffic-related sources, and the rooftop can be considered as an urban background with significantly reduced exposure to air pollutants from ground-based sources. Particle samples were collected on five consecutive days in September 2006 (September 21–26, 2006), five consecutive days in October 2006 (October 17–22, 2006), and six consecutive days in January 2007 (January 5–11). Visibility data indicated good visibility on the September sampling days (visibility: 18–36 km) and low visibility on the October and January sampling days (visibility: <10 km). Two high-volume $PM_{2.5}$ samplers (Graseby Anderson, Atlanta, GA, USA) was used to collect $PM_{2.5}$ particles on quartz filters (Whatman, Mainstone, UK) at a flow rate of 1.13 m^3 min^{-1}. Each sample was collected for 24-h. Before field use, filters were previously annealed in a muffle furnace for 12 h at 450 °C, wrapped in aluminum foil and zipped in Teflon® bags. After sample collection, filters were again wrapped in aluminum foil, zipped in polytetrafluoroethylene bags, and stored in a refrigerator at −18 °C until analysis.

2.2. Chemical analysis

The organic and element carbon (OC/EC) concentrations were measured using a thermal–optical method described by Zhang et al. (2010). Three punches, 1.5 × 1.0 cm a punch, of each filter were extracted in 20 mL of 18-MOhm MilliQ water and sonicated for 30 min in an ice-water bath. After filtered, the extract was analyzed for K^+ and sulfate using ion chromatography (Metrohm 883, Herisau, Switzerland).

A mixture of five isotopically labeled PAH compounds (naphthalene-d8, acenaphthene-d10, phenanthrene-d10, chrysene-d12, and perylene-d12), tetracosane-d50 and levoglucosan-$^{13}C_6$ were added as surrogates prior to extraction. Samples were ultrasonically extracted twice with 40 mL hexane, then three times with 40 mL dichloromethane (DCM)/methanol (1:1, v/v). The extracts were concentrated to 1 mL and split into two aliquots. One aliquot (~0.5 mL) was solvent-exchanged to redistilled hexane, and then purified using a 1:2 alumina/silica column chromatography. Two fractions were eluted. The first fraction containing nonpolar compounds was eluted by 30 mL of hexane. The second fraction was eluted by 70 mL of DCM/hexane (3:7 v/v). The two fractions were combined, concentrated to ~2 mL and blown to dryness under a gentle stream of nitrogen. This was redissolved with n-hexane to ~0.5 mL and analyzed for PAHs and hopanes. The other aliquot (~0.5 mL) was blown to dryness for silylation with 100 μL of pyridine and 200 μL of BSTFA (BSTFA/TMCS, 99:1, Supelco) in an oven at 70 °C for 1 h. The silylated extract was then analyzed for levoglucosan.

The samples were analyzed using an Agilent GC–MS (6890-5973N) equipped with a DB-5MS column (50 m × 0.32 mm × 0.17 μm). The column temperature was initiated at 80 °C (held for 2 min) and increased to 290 °C at 4 °C min^{-1} (held for 30 min). An aliquot of 1 μL was injected in splitless/split mode with a solvent delay of 6 min. Target compounds were identified based on their mass spectra and retention times. Molecular ions, m/z 191 and m/z 60 were used as target ions for the quantification of PAHs, hopanes and levoglucosan, respectively.

In this study, PAH compounds are given abbreviations as follows: naphthalene (Nap), acenaphthylene (Acey), acenaphthene

(Ace), fluorene (Fl), phenanthrene (Phe), anthracene (Ant), fluoranthene (Flu), pyrene (Pyr), benz[a]anthracene (BaA), chrysene (Chr), benzo[b]fluoranthene (BbF), benzo[k]fluoranthene (BkF), benzo[e]pyrene (BeP), benzo[a]pyrene (BaP), indeno[1,2,3-cd]pyrene (IcdP), benzo[g,h,i]perylene (BghiP), dibenz[a,h]anthracene (DahA) and Coronene (Cor).

Field blanks and lab blanks were routinely analyzed to determine any background contamination. All results showed very low analytes and in most cases not detectable in the blanks. Recovery efficiencies were determined by evaluating surrogate recovery standards spiked to the samples. The mean recoveries for surrogates in field samples were naphthalene-d8 34%, acenaphthalene-d8 42%, phenanthrene-d10 39%, chrysene-d12 90%, perylene-d12 67% and levoglucosan-$^{13}C_6$ 87%.

3. Results and discussion

3.1. Concentrations of polycyclic aromatic hydrocarbons

Table 1 reports the mean concentrations of individual PAHs in $PM_{2.5}$ collected at the rooftop (RF) and the roadside (RS) in September, October and January. The total concentrations of PAHs were in the range of 7.4–41.8 ng m^{-3}. The mean concentrations of PAHs in the combined RF and RS sample sets were the lowest in September (12.2 ng m^{-3}), higher in October (17.8 ng m^{-3}) and the highest in January (28.4 ng m^{-3}). There are several contributing factors to this temporal trend. In cold periods, more PAHs, particularly smaller PAHs, were partitioned onto fine particles (Chetwittayachan et al., 2002; Panther et al., 1999). The southeast wind in the autumn shifting to the northeast wind in the winter also brought polluted air masses from northern China. Enhanced biomass burning and less photodegradation of PAHs further contributed to the higher level of PAHs in January. The PAH concentrations observed in this study were comparable to those in previous studies conducted in Guangzhou (Bi et al., 2003; Li et al., 2006) and Shenzhen (Liu et al., 2010), another large city in the PRD, but higher than those in other urban areas reported in the world (Baek et al., 1991; Eiguren-Fernandez et al., 2004; Sklorz et al., 2007).

We also found larger proportion of high molecular weight (HMW) PAHs than their smaller homologs in the $PM_{2.5}$ samples. The mean concentrations of PAHs with 2–3 aromatic rings were 3.0 ng m^{-3}, while those with 5–7 rings were elevated to 10.8 ng m^{-3}. As a result, PAHs of 5–7 rings accounted for 35–76% of the total concentrations and PAHs of 2–3 rings accounted for 9–22%. The low concentrations of small PAHs were consistent with their physiochemical properties. With high vapor pressure and high volatility, these compounds existed primarily in the gaseous phase (Re-Poppi and Santiago-Silva, 2005; Tsapakis and Stephanou, 2005a,b). Significantly higher ($p < 0.01$, t-test) loadings of the four-ring PAHs were found in January (40% on average) than those in September and October (21% on average). Atmospheric temperature significantly affects the distribution of PAHs between the gas and particle phases and the low ambient temperature in winter resulted in a relatively larger portion of PAHs partitioning to the particle phase.

To evaluate the change of PAH compositions during haze periods, the ratios of individual PAHs at the RF and the RS in haze and non-haze periods were shown in Fig. 1. The ratios of the individual PAH concentration at the RF to that at the RS (RF/RS), especially for the HMW PAHs, were less than 0.6 in the September samples, which were collected on days of good visibility. In October and January, also coinciding with haze periods, however, most of the RF/RS ratios were larger than 0.6. The 4–6 ring PAHs, namely BaA, Chr, BbF, BkF, BaP, InP, DBA and BghiP, are considered to have carcinogenic effects (Yassaa et al., 2001). This indicated that the composition of PAHs were significantly different on haze and non-haze days. Larger proportions of higher ring PAHs on haze days

Table 1
Average concentrations (ng m^{-3}) of $PM_{2.5}$-bound PAHs in urban Guangzhou in three sampling months.

	Diagnostic ion (m/z)	September		October		January	
		28.6–29.3 °C		27.6–28.7 °C		17.3–21.1 °C	
		Rooftop	Roadside	Rooftop	Roadside	Rooftop	Roadside
Nap	128 (2)[a]	0.40	0.56	0.47	0.67	0.27	0.30
Acey	152 (3)	0.08	0.12	0.14	0.12	0.16	0.33
Ace	154 (3)	0.04	0.05	0.03	0.05	0.06	0.06
Fl	166 (3)	0.07	0.09	0.09	0.11	0.10	0.10
Phe	178 (3)	0.67	1.16	0.81	1.08	3.62	3.82
Ant	178 (3)	0.08	0.16	0.14	0.17	0.05	0.08
Flu	202 (4)	0.53	0.84	0.62	0.78	4.34	4.03
Pyr	202 (4)	0.63	0.97	0.68	0.92	3.54	3.48
BaA[b]	228 (4)	0.26	0.42	0.41	0.49	0.91	0.98
Chr[b]	228 (4)	0.54	0.86	0.96	1.14	2.66	2.91
BbF[b]	252 (5)	1.21	2.47	2.71	3.16	3.58	3.75
BkF[b]	252 (5)	1.32	2.24	3.10	2.56	2.89	2.81
BeP	252 (5)	1.10	2.08	2.38	2.48	2.43	2.70
BaP[b]	252 (5)	0.59	1.06	1.33	1.48	1.56	1.82
IcdP[b]	276 (6)	0.53	0.99	0.92	0.93	0.71	0.76
BghiP	276 (6)	0.64	1.23	1.12	1.16	0.72	0.79
DahA[b]	278 (5)	0.06	0.11	0.17	0.17	0.19	0.18
Cor	300 (7)	0.09	0.18	0.15	0.15	0.08	0.10
$\sum$PAHs		8.83	15.61	17.93	17.59	27.87	29.01
$\sum_4$Hopanes[c]		1.11	6.93	3.00	4.18	2.28	4.26
Levoglucosan		39.51	52.52	65.71	77.32	166.81	172.83
EC (μg m^{-3})		4.18	6.74	4.38	5.52	2.89	4.43
OC (μg m^{-3})		11.38	21.92	18.70	22.09	16.83	21.54
K^+ (μg m^{-3})		0.83	1.29	1.12	0.92	3.01	2.95
Sulfate (μg m^{-3})		23.35	25.63	26.52	31.34	24.72	23.99

[a] The numbers in brackets represent the number of rings.
[b] EPA Class B2 carcinogens.
[c] The four hopanes are 17α(H)-21β(H)-29-Norhopane, 17α(H)-21β(H)-Hopane, 22S-Homohopane and 22R-Homohopane.

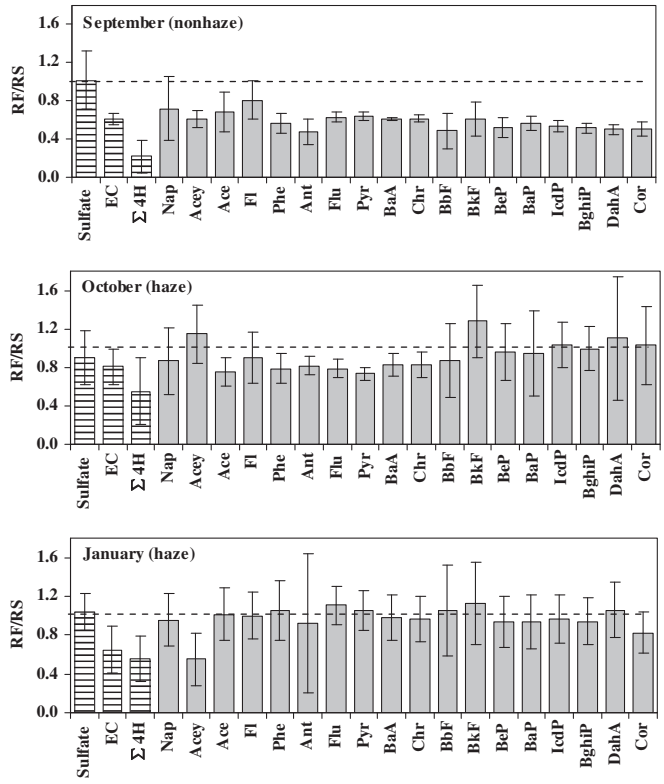

Fig. 1. The concentration ratios between rooftop and roadside samples for individual PAHs, sulfate, EC and $\sum_4$Hopanes in $PM_{2.5}$ in the three sampling months.

suggested more potential risk for human health associated with the PM encountered under the low visibility conditions.

3.2. Carcinogenic potency of PAHs

BaP, known as the most carcinogenic PAH, is the most investigated PAH and often used as an indicator of the carcinogenicity of the total PAHs. The BaP levels in $PM_{2.5}$ collected in this study ranged from 0.45 to 3.2 ng m^{-3}. It is worth noting that on most of the haze days, BaP levels exceeded 1 ng m^{-3}, the WHO air quality guideline recommended for BaP as daily average. The BaP levels were lower in September, medium in October and relatively high in January, showing a similar trend as those for the total PAHs.

For the assessment of the carcinogenic potency of PAHs, carcinogenic PAHs adjusted by their cancer potency equivalence factors (BaP_{eq}) were calculated using the following equation:

$$BaP_{eq} = BaA \times 0.06 + BF \times 0.07 + BaP + DahA \times 0.6 + IcdP \times 0.08$$

The cancer potency equivalency factors (PEF) proposed by Yassaa et al. (Yassaa et al., 2001) were used. In this scheme, BaP was used as a reference compound and assigned a PEF value of 1. BaP_{eq} values for individual sampling days at the RF and the RS are presented in Fig. 2. The mean concentrations of BaP_{eq} in $PM_{2.5}$ were 1.93 ng m^{-3}.

We compared BaP_{eq} between samples from the RF and the RS. As can be seen in Fig. 2, during the non-haze days, the RS $PM_{2.5}$ showed higher levels of BaP_{eq} than the RF $PM_{2.5}$ ($p < 0.05$, t-test). During haze days, however, BaP_{eq} of the RF $PM_{2.5}$ were drastically elevated and became comparable to those of RS samples. Such a difference in BaP_{eq} between non-haze and haze days implied that during haze episodes, the public in the urban area was exposed to carcinogenic PAHs as much as in the polluted roadside

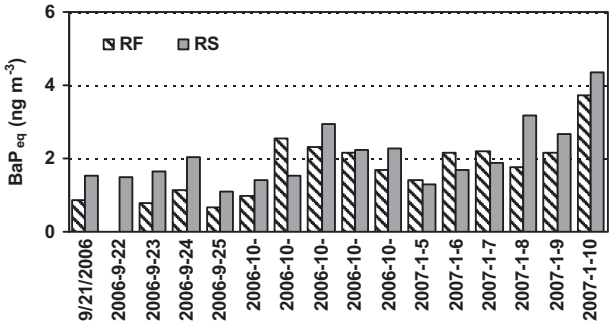

Fig. 2. Daily variations of BaP_{eq} in the rooftop (RF) and roadside (RS) samples.

microenvironment. This result was consistent with previous genotoxic test, which concluded that genotoxic potencies at RF were as serious as those at RS on haze days (Xu et al., 2008).

3.3. Source identification of PAHs

The significant combustion sources influencing PAHs in urban Guangzhou are expected to include vehicular emissions, industrial coal combustion for power generation, and biomass burning. Coal combustion is the principal energy source in power plants in South China (Li et al., 2006); however, residential heating normally is not necessary in cities in South China therefore, emissions from domestic coal burning are negligible in this region. For Guangzhou specifically, the consumption data for industrial coal, gasoline and diesel in 2006 were 14.1, 4.4 and 6.2 million tons, respectively. The biomass consumption, without published data, was estimated to be 9.2 million tons based on the regression model for biomass fuel consumption provided by Xu et al. (2006). Together with energy emission factors provided by the same authors, the emission rates of total PAHs in 2006 were calculated to be 328 tons (85.7%) from biomass burning emissions, 54 tons (14.1%) from vehicular emissions, 0.7 tons (0.2%) from industrial coal combustion, respectively.

Estimation from the emission inventory indicates biomass burning to be a considerable source of PAHs. Crop residue burning is the main form of open biomass burning in the PRD (Lin et al., 2010). Levoglucosan has been used as a tracer for biomass burning in general (Fraser and Lakshmanan, 2000; Simoneit, 2002; van Drooge and Ballesta, 2009). The influence of biomass burning is clearly seen in the presence of significant levels of levoglucosan in our samples. The average level of levoglucosan was 46.7 ng m^{-3} in September, 71.5 ng m^{-3} in October, and 169.8 ng m^{-3} in January.

Among the major combustion sources, vehicular emissions had a significant local contribution at our sampling site while the other two sources are regional. Concurrent sampling at the roadside and on the 50-m high rooftop at the same location provides an opportunity to evaluate the relative importance between the local vehicular emissions and the regional combustion sources. The regional sources would influence roadside and rooftop to the same extent while local vehicular emissions would impact the roadside more than the rooftop.

Molecular tracers are indicative of their emission sources and formation pathways. To examine the relative influence of local vehicular emissions and regional PM sources, we used the following tracers: EC and hopanes for vehicular sources and sulfate for secondary and regional sources. Daily variations of these three species are plotted in Fig. S2. Different hopane compounds were highly correlated ($R^2 > 0.85$). The sum concentrations of the four most abundant hopanes, denoted as $\sum_4$hopanes, are shown in Fig. S2. As expected, EC and hopanes consistently showed lower

concentrations at RF than those at RS. The EC level was 21–38% lower and the $\sum_4$hopanes level was 28–84% lower in the RF samples. In comparison, sulfate did not show much difference between RF and RS samples. Together with the distinct vertical spatial distribution of PAHs on haze and non-haze days (Fig. S3), it is reasonable to infer that the local vehicular sources had a significant influence on PAH levels on the non-haze days (September), whereas PAHs on haze days (October and January) were dominated by regional PM sources.

Linear regression analyses on the concentrations of individual PAHs, excluding Nap due to its high volatility and Ant and BaA due to their high degradation, were carried out to identify groups of PAHs that have common sources. Three groups of PAHs are found to have strong correlations with correlation coefficients $r^2 > 0.80$: (1) Phe, Flu, Pyr, and Chr, (2) BbF, BeP, BaP, and DahA, and (3) BghiP, IcdP, and Cor. These results indicated that PAHs with comparative ring sizes have similar sources and PAHs with distinct ring sizes have different sources. Select pairs of PAHs in each group are examined below for source identification.

Flu/Pyr and IcdP/BghiP were selected because they photolytically degrade at comparable rates (Ding et al., 2007; Yunker et al., 2002). BaP/BeP was used to explore the influence of photochemical aging as BaP degrades faster than BeP. Simple scatter plots of the three pairs of PAHs are shown in Fig. 3 to visualize the measured ambient PAH data in this study and PAH data previously reported for another two locations in urban Guangzhou (Li et al., 2006; Yang et al., 2010). Also shown are published source profiles for vehicle emissions, biomass burning and coal combustion (He et al., 2008; Sheesley et al., 2003; Yu and Yu, 2011; Zhang et al., 2008). The vehicle emission composition is from data collected in Zhujiang Tunnel in the western urban area of Guangzhou (He et al., 2008). The biomass burning profiles are measured data of rice straw burning emissions obtained in open field burning in the PRD (Yu and Yu, 2011) and in dilution chamber measurements (Sheesley et al., 2003) and sugarcane burning in the PRD (Yu and Yu, 2011). The coal combustion profiles are selected from industrial coal combustion with coal from the main coal-mining regions in China (Zhang et al., 2008).

The previously reported Guangzhou urban PAH data were annual average data in 2001/2002 (Li et al., 2006) and in 2005/2006 (Yang et al., 2010) since individual sample data were not reported in their papers. The Pyr/Flu and BghiP/IcdP ratios obtained in the two previous studies were similar to those measured in this work (Fig. 3a and b), possibly reflecting the main combustion sources had not changed over the different study periods.

The Pyr/Flu ratios in September and October were close to that of vehicular emissions while the ambient ratios in January were lower than that of vehicular emissions and close to those of rice straw/sugarcane burning and industrial coal combustion (Fig. 3a). Such a seasonal variation in Pyr/Flu ratio suggests significant vehicular contribution to these two PAHs in September and October and shift of the dominant source to regional combustion sources in January.

The BghiP/IcdP ratios were similar among the three sampling months (Fig. 3b). They are close to those of rice straw/sugarcane burning and industrial coal combustion but significantly lower than the ratio measured in the Zhujiang Tunnel, indicating that traffic could not be the dominant contributor to these two PAHs. The BghiP/IcdP ratios of industrial coal emissions bracket those of rice straw/sugarcane burning emissions, making it impossible to rely on the BghiP/IcdP ratio to distinguish between these two types of regional combustion sources.

Fig. 3c showed the scatter plot of BaP versus BeP for ambient data and source profiles. The ambient BaP/BeP data were much lower than those of rice straw/sugarcane leave combustion emissions; instead, they were between those of vehicular emissions and industrial coal (bituminite) combustion emissions. The average BaP/BeP ratios were 0.52 ± 0.09 in September, 0.57 ± 0.09 in October and 0.65 ± 0.09 in January. This could be either indicative of some photochemical aging or the seasonal variation in source contributions. Biomass profiles have higher BaP/BeP and more contribution of biomass burning could be a factor for the larger BaP/BeP in the January ambient data. This example also demonstrates that it is problematic to rely on BaP/BeP ratio to infer the degree of photochemical aging.

Scatter plots have limitations though, PAHs emitted by two or more source classes are expected to create scattered plots and therefore it is more difficult to interpret. Furthermore, multiple source profiles are available for each source class as a result of varying combustion conditions and fuel compositions. In comparison, ratio–ratio plots, which include a third stable reference compound, are capable of clearly visualizing ambient molecular marker data and multiple source profile data. In addition, these plots allow qualitative evaluation of mixing of emissions from different

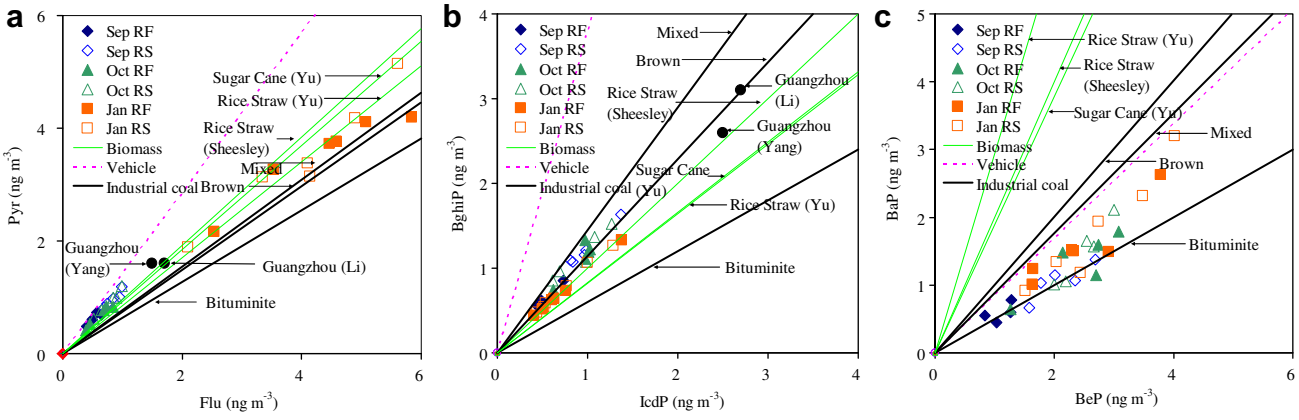

Fig. 3. Scatter plots of (a) pyrene versus fluoranthene, (b) Benzo[ghi]perylene versus indeno[1,2,3-cd]pyrene, and (c) benzo[a]pyrene versus benzo[e]pyrene. The lines are published source profiles taken from the literature (He et al., 2008; Sheesley et al., 2003; Yu and Yu, 2011; Zhang et al., 2008). The vehicular emission composition is from data collected in Zhujiang Tunnel in the western urban area of Guangzhou (He et al., 2008). The biomass burning profiles are measured data of rice straw burning emissions obtained in open field burning in the PRD (Yu and Yu, 2011) and in dilution chamber measurements (Sheesley et al., 2003) and sugarcane burning in the PRD (Yu and Yu, 2011). The coal combustion profiles are selected from industrial coal combustion in the main coal-mining regions in China (Zhang et al., 2008). Also shown are previous annual average concentration data measured in urban Guangzhou (Li et al., 2006; Yang et al., 2010).

sources and assessing possible photochemical aging (Robinson et al., 2006). The principle of the ratio–ratio plots was detailed by Robinson et al. (Robinson et al., 2006). In brief, ambient data that cluster to a point on a ratio–ratio plot can be described by a single source profile or potentially multiple sources with fixed source strengths. Ambient data distributing along a diagonal that extends toward the lower-left-hand corner of the plot indicate photochemical aging. Ambient data that organize along a line in a ratio–ratio plot indicate the existence of two sources with varying source strengths. Ambient data scattering on a ratio–ratio plot indicate three or more source classes with varying strengths. A key to construct ratio–ratio plot is to select proper compounds. In this paper, we chose EC as the reference compound because it is chemically stable in the ambient atmosphere and vehicular emissions can be regarded as its dominant sources in this region (Hagler et al., 2006; Yu and Yu, 2011). BghiP and IcdP are selected because they predominantly exist in the particle phase in all three sampling months and have been previously used as molecular markers in source apportionment analysis (Harrison et al., 1996; Larsen and Baker, 2003).

Fig. 4a shows the ratio–ratio plot of BghiP and IcdP normalized by EC. The vehicle profile derived from the tunnel measurements in Guangzhou (He et al., 2008) has significantly lower PAH-to-EC ratios than the industrial coal combustion profiles and the rice straw/sugarcane leave burning emissions are in-between. The ambient data lie close to those of rice straw/sugarcane leave burning emissions and organize along a line that extends from the biomass burning source profile toward the lower-left-hand corner. Among the ambient data, the January data are closer to the biomass burning profiles than those in September and October. This was consistent with higher concentration of K^+ and levoglucosan in January than the other two months (Table 1). The MODIS fire maps also show many more fire spots in January 2007 than in September 2006 (http://firefly.geog.umd.edu/firemap/) (Fig. S4). The scatter plot (Fig. 3b) and the ratio–ratio plot (Fig. 4) are consistent in indicating biomass burning dominated the ambient concentrations of the two PAHs.

3.4. Photochemical aging

During atmospheric transport, PAH compounds are exposed to O_3, OH, NO_2 and other potential oxidants that degrade PAHs to various extents and thereby change the relative composition of PAHs (Brubaker and Hites, 1998; Esteve et al., 2006; Liu et al., 2006; Schauer et al., 2003; Tsapakis and Stephanou, 2003). While PAH compounds decay in the ambient atmosphere, EC is chemically stable. Therefore, photochemical degradation of PAHs would reduce the PAH-to-EC ratio in the ambient air compared to fresh emissions. In Fig. 4a, the PAH data spread along a 1:1 line and lower PAH-to-EC ratios were observed in September than those in October and January. These can be explained by either more extensive photochemical oxidation in September or source–source mixing, of which the mixing line distributed along the diagonal. It is not possible to distinguish these two processes by examining the PAH/EC ratio–ratio plots alone. However, evidence of significant photooxidation of aerosol phase hopanes, with vehicular emissions as the predominant source in urban areas, could be inferred from ratio–ratio plots.

A ratio–ratio plot similar to the PAH/EC ratio–ratio plot was constructed for norhopane and hopane (Fig. 4b). The source profiles for vehicle emissions and industrial coal combustion were also shown on the plot. The norhopane/EC and hopane/EC for Zhujiang tunnel are 0.31 and 0.57 ng μg^{-1}, respectively. The two ratios have average values of 1.4 and 16 ng μg^{-1} in the industrial coal combustion source profiles. The two ratios in the RS samples were on average 0.27 and 0.45, respectively, significantly lower than that of coal combustion emissions. The ratios were only slightly lower than that measured in the tunnel, suggesting vehicular emissions as their dominant source. The homohopane index $[S/(S+R)]$ was 0.53 ± 0.03 in the RS ambient data, in line with the typical value (0.6) for petroleum (Seifert and Moldowan, 1978) rather than for coal smoke samples (0.05–0.35) (Oros and Simoneit, 2000), further confirming vehicles as the dominant source for the hopanes. The average values of the two ratios in the RF samples were 0.18 and 0.28, respectively, lower than those in the RS samples. The lower ratios in the ambient samples indicate faster loss of particle hopanes than EC in the atmosphere after their emissions, that is, the photochemical oxidation of hopanes. Air masses sampled at the RF contained more aged vehicular emissions and less fresh traffic emissions than the RS location. Consequently, the average extent of photochemical degradation of hopanes on the rooftop was more than those experienced at the roadside.

We next use $\sum_4$Hopanes/EC to evaluate the contribution of aging. The $\sum_4$Hopanes/EC in Zhujiang Tunnel is 1.14 ng μg^{-1}, which could be approximated as the value of fresh emission. The values of

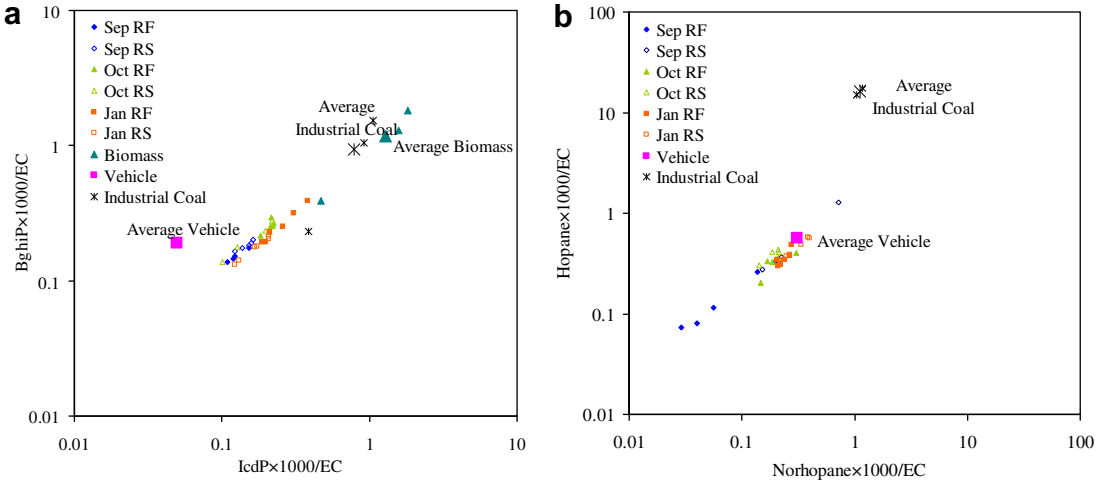

Fig. 4. Ratio–ratio plot of (a) BghiP and IcdP and (b) hopane and norhorpane normalized by EC. The vehicular emission composition is from data collected in Zhujiang Tunnel in the western urban area of Guangzhou (He et al., 2008). The biomass burning profiles are measured data of rice straw burning emissions obtained in open field burning in the PRD (Yu and Yu, 2011) and in dilution chamber measurements (Sheesley et al., 2003) and sugarcane burning in the PRD (Yu and Yu, 2011). The coal combustion profiles are selected from industrial coal combustion in the main coal-mining regions in China (Zhang et al., 2008).

$\sum_4$Hopanes/EC for RF and RS samples were 0.28|1.06 in September, 0.69|0.76 in October, and 0.78/0.95 in January. All the ambient $\sum_4$Hopanes/EC ratios were significantly lower than those measured in the tunnel, indicating that considerable photooxidation of hopanes had occurred after their emissions. The higher ratios in the RS samples reflect the higher contributions of fresh vehicular emissions due to the proximity of the sampling point to traveling vehicles. The highest extent of photooxidation of hopanes was observed in the rooftop samples in September, followed by those in October and in January. This order is consistent with the expected seasonality of photochemical activities.

4. Summary

In an urban Guangzhou location, $PM_{2.5}$ aerosol samples were collected simultaneously at roadside and on rooftop. Vehicular emissions as a significant local PM source were confirmed by the consistently lower elemental carbon and hopane concentrations in the rooftop samples than the roadside samples. Regional PM components such as sulfate, on the other hand, had little vertical spatial gradient, indicating regional PM sources impact the roadside and the rooftop to similar extents. The total PAHs concentrations measured was ~43% lower at the rooftop on sampling days in September 2006 (coinciding with good visibility days) but similar in October 2006 and in January 2007 (coinciding with haze days). Ambient PAH data were compared with relevant source profiles including roadway tunnel data, rice straw/sugarcane leave combustion emissions, and industrial coal combustions to identify dominating sources. The source analysis indicates that the 4-ring PAHs such as pyrene and fluoranthene had a shift in their dominating source from vehicular emissions in September and October to regional combustion source in January. A few major 5- and 6-ring PAHs such as benzo[ghi]perylene and indeno[1,2,3-cd]pyrene were more likely dominated by regional biomass burning emissions. A more quantitative source apportionment was not possible due to the limited number of samples and possible photodegradation of molecular source tracers.

Cancer risk of the carcinogenic PAHs in term of benzo(a)pyrene-equivalent carcinogenic potency (BaP_{eq}) was compared for the rooftop and the roadside samples. On the haze sampling days (the October and January samples), the BaP_{eq} values in the rooftop samples were comparable to those in the roadside samples. This is a result of regional combustion sources dominating the carcinogenic PAHs, which in turn suggests controlling regional combustion sources is important in reducing health risk related to exposure to PAHs in urban $PM_{2.5}$ in Guangzhou.

Acknowledgments

This study was financially supported by the National Natural Science Foundation of China (Project No. 40821003/41025012).

Appendix. Supplementary material

Supplementary data related to this article can be found online at doi:10.1016/j.atmosenv.2011.09.005.

References

Baek, S.O., Goldstone, M.E., Kirk, P.W.W., Lester, J.N., Perry, R., 1991. Phase distribution and particle-size dependency of polycyclic aromatic-hydrocarbons in the urban atmosphere. Chemosphere 22, 503–520.

Bi, X.H., Sheng, G.Y., Peng, P., Chen, Y.J., Zhang, Z.Q., Fu, J.M., 2003. Distribution of particulate- and vapor-phase n-alkanes and polycyclic aromatic hydrocarbons in urban atmosphere of Guangzhou, China. Atmos. Environ. 37, 289–298.

Brubaker, W.W., Hites, R.A., 1998. OH reaction kinetics of polycyclic aromatic hydrocarbons and polychlorinated dibenzo-p-dioxins and dibenzofurans. J. Phys. Chem. A 102, 915–921.

Chetwittayachan, T., Shimazaki, D., Yamamoto, K., 2002. A comparison of temporal variation of particle-bound polycyclic aromatic hydrocarbons (pPAHs) concentration in different urban environments: Tokyo, Japan, and Bangkok, Thailand. Atmos. Environ. 36, 2027–2037.

Deng, X.J., Tie, X.X., Wu, D., Zhou, X.J., Bi, X.Y., Tan, H.B., Li, F., Hang, C.L., 2008. Long-term trend of visibility and its characterizations in the Pearl River Delta (PRD) region, China. Atmos. Environ. 42, 1424–1435.

Ding, X., Wang, X.M., Xie, Z.Q., Xiang, C.H., Mai, B.X., Sun, L.G., Zheng, M., Sheng, G.Y., Fu, J.M., Poschl, U., 2007. Atmospheric polycyclic aromatic hydrocarbons observed over the North Pacific Ocean and the Arctic area: spatial distribution and source identification. Atmos. Environ. 41, 2061–2072.

Eiguren-Fernandez, A., Miguel, A.H., Froines, J.R., Thurairatnam, S., Avol, E.L., 2004. Seasonal and spatial variation of polycyclic aromatic hydrocarbons in vapor-phase and $PM_{2.5}$ in Southern California urban and rural communities. Aerosol. Sci. Technol. 38, 447–455.

Esteve, W., Budzinski, H., Villenave, E., 2006. Relative rate constants for the heterogeneous reactions of NO_2 and OH radicals with polycyclic aromatic hydrocarbons adsorbed on carbonaceous particles. Part 2: PAHs adsorbed on diesel particulate exhaust SRM 1650a. Atmos. Environ. 40, 201–211.

Fraser, M.P., Lakshmanan, K., 2000. Using levoglucosan as a molecular marker for the long-range transport of biomass combustion aerosols. Environ. Sci. Technol. 34, 4560–4564.

Hagler, G.S., Bergin, M.H., Salmon, L.G., Yu, J.Z., Wan, E.C.H., Zheng, M., Zeng, L.M., Kiang, C.S., Zhang, Y.H., Lau, A.K.H., Schauer, J.J., 2006. Source areas and chemical composition of fine particulate matter in the Pearl River Delta region of China. Atmos. Environ. 40, 3802–3815.

Harrison, R.M., Smith, D.J.T., Luhana, L., 1996. Source apportionment of atmospheric polycyclic aromatic hydrocarbons collected from an urban location in Birmingham, UK. Environ. Sci. Technol. 30, 825–832.

He, L.Y., Hu, M., Zhang, Y.H., Huang, X.F., Yao, T.T., 2008. Fine particle emissions from on-road vehicles in the Zhujiang Tunnel, China. Environ. Sci. Technol. 42, 4461–4466.

Hu, M., Zhao, Y.L., Slanina, S., Zhang, Y.H., 2007. Chemical compositions of fine particulate organic matter emitted from Chinese cooking. Environ. Sci. Technol. 41, 99–105.

Larsen, R.K., Baker, J.E., 2003. Source apportionment of polycyclic aromatic hydrocarbons in the urban atmosphere: a comparison of three methods. Environ. Sci. Technol. 37, 1873–1881.

Li, J., Zhang, G., Li, X.D., Qi, S.H., Liu, G.Q., Peng, X.Z., 2006. Source seasonality of polycyclic aromatic hydrocarbons (PAHs) in a subtropical city, Guangzhou, South China. Sci. Total Environ. 355, 145–155.

Lin, P., Engling, G., Yu, J.Z., 2010. Humic-like substances in fresh emissions of rice straw burning and in ambient aerosols in the Pearl River Delta Region, China. Atmos. Chem. Phys. 10, 6487–6500.

Liu, G.Q., Tong, Y.P., Luong, J.H.T., Zhang, H., Sun, H.B., 2010. A source study of atmospheric polycyclic aromatic hydrocarbons in Shenzhen, South China. Environ. Monit. Assess. 163, 599–606.

Liu, Y., Sklorz, M., Schnelle-Kreis, J., Orasche, J., Ferge, T., Kettrup, A., Zimmermann, R., 2006. Oxidant denuder sampling for analysis of polycyclic aromatic hydrocarbons and their oxygenated derivates in ambient aerosol: evaluation of sampling artefact. Chemosphere 62, 1889–1898.

Mai, B.X., Qi, S.H., Zeng, E.Y., Yang, Q.S., Zhang, G., Fu, J.M., Sheng, G.Y., Peng, P.N., Wang, Z.S., 2003. Distribution of polycyclic aromatic hydrocarbons in the coastal region off Macao, China: assessment of input sources and transport pathways using compositional analysis. Environ. Sci. Technol. 37, 4855–4863.

Marr, L.C., Dzepina, K., Jimenez, J.L., Reisen, F., Bethel, H.L., Arey, J., Gaffney, J.S., Marley, N.A., Molina, L.T., Molina, M.J., 2006. Sources and transformations of particle-bound polycyclic aromatic hydrocarbons in Mexico City. Atmos. Chem. Phys. 6, 1733–1745.

Oros, D.R., Simoneit, B.R.T., 2000. Identification and emission rates of molecular tracers in coal smoke particulate matter. Fuel 79, 515–536.

Panther, B.C., Hooper, M.A., Tapper, N.J., 1999. A comparison of air particulate matter and associated polycyclic aromatic hydrocarbons in some tropical and temperate urban environments. Atmos. Environ. 33, 4087–4099.

Poster, D.L., Hoff, R.M., Baker, J.E., 1995. Measurement of the particle-size distributions of semivolatile organic contaminants in the atmosphere. Environ. Sci. Technol. 29, 1990–1997.

Re-Poppi, N., Santiago-Silva, M., 2005. Polycyclic aromatic hydrocarbons and other selected organic compounds in ambient air of Campo Grande City, Brazil. Atmos. Environ. 39, 2839–2850.

Robinson, A.L., Subramanian, R., Donahue, N.M., Bernardo-Bricker, A., Rogge, W.F., 2006. Source apportionment of molecular markers and organic aerosols-1. Polycyclic aromatic hydrocarbons and methodology for data visualization. Environ. Sci. Technol. 40, 7803–7810.

Schauer, C., Niessner, R., Poschl, U., 2003. Polycyclic aromatic hydrocarbons in urban air particulate matter: decadal and seasonal trends, chemical degradation, and sampling artifacts. Environ. Sci. Technol. 37, 2861–2868.

Seifert, W.K., Moldowan, J.M., 1978. Applications of steranes, terpanes and monoaromatics to maturation, migration and source of crude oils. Geochim. Cosmochim. Acta 42, 77–95.

Sheesley, R.J., Schauer, J.J., Chowdhury, Z., Cass, G.R., Simoneit, B.R.T., 2003. Characterization of organic aerosols emitted from the combustion of biomass indigenous to South Asia. J. Geophys. Res-Atmos. 108.

Simoneit, B.R.T., 2002. Biomass burning – a review of organic tracers for smoke from incomplete combustion. Appl. Geochem. 17, 129–162.
Sklorz, M., Schnelle-Kreis, J., Liu, Y.B., Orasche, J., Zimmermann, R., 2007. Daytime resolved analysis of polycyclic aromatic hydrocarbons in urban aerosol samples – impact of sources and meteorological conditions. Chemosphere 67, 934–943.
Tsapakis, M., Stephanou, E.G., 2003. Collection of gas and particle semi-volatile organic compounds: use of an oxidant denuder to minimize polycyclic aromatic hydrocarbons degradation during high-volume air sampling. Atmos. Environ. 37, 4935–4944.
Tsapakis, M., Stephanou, E.G., 2005a. Occurrence of gaseous and particulate polycyclic aromatic hydrocarbons in the urban atmosphere: study of sources and ambient temperature effect on the gas/particle concentration and distribution. Environ. Pollut. 133, 147–156.
Tsapakis, M., Stephanou, E.G., 2005b. Polycyclic aromatic hydrocarbons in the atmosphere of the Eastern Mediterranean. Environ. Sci. Technol. 39, 6584–6590.
van Drooge, B.L., Ballesta, P.P., 2009. Seasonal and daily source apportionment of polycyclic aromatic hydrocarbon concentrations in PM_{10} in a Semirural European area. Environ. Sci. Technol. 43, 7310–7316.
Wang, B.G., Yang, J.H., Zhou, Y., Feng, Z.C., Liu, H.X., 2008. The emission characteristics of metal elements in urban motor vehicles exhaust of Gnangzhou City. China Environ. Sci. 28, 389–394.
Wu, D., Tie, X.X., Li, C.C., Ying, Z.M., Lau, A.K.H., Huang, J., Deng, X.J., Bi, X.Y., 2005. An extremely low visibility event over the Guangzhou region: a case study. Atmos. Environ. 39, 6568–6577.
Xu, H.J., Wang, X.M., Poesch, U., Feng, S.L., Wu, D., Yang, L., Li, S.X., Song, W., Sheng, G.Y., Fu, J.M., 2008. Genotoxicity of total and fractionated extractable organic matter in fine air particulate matter from urban Guangzhou: comparison between haze and non-haze episodes. Environ. Toxicol. Chem. 27, 206–212.
Xu, S.S., Liu, W.X., Tao, S., 2006. Emission of polycyclic aromatic hydrocarbons in China. Environ. Sci. Technol. 40, 702–708.
Yang, F., Zhai, Y.B., Chen, L., Li, C.T., Zeng, G.M., He, Y.D., Fu, Z.M., Peng, W.F., 2010. The seasonal changes and spatial trends of particle-associated polycyclic aromatic hydrocarbons in the summer and autumn in Changsha city. Atmos. Res. 96, 122–130.
Yassaa, N., Meklati, B.Y., Cecinato, A., Marino, F., 2001. Particulate n-alkanes, n-alkanoic acids and polycyclic aromatic hydrocarbons in the atmosphere of Algiers City Area. Atmos. Environ. 35, 1843–1851.
Yu, H., Yu, J.Z., 2011. Size distributions of polycyclic aromatic hydrocarbons at two receptor sites in the Pearl River Delta region, China: implications of a dominant droplet mode. Aerosol. Sci. Technol. 45, 101–112.
Yunker, M.B., Macdonald, R.W., Vingarzan, R., Mitchell, R.H., Goyette, D., Sylvestre, S., 2002. PAHs in the Fraser River basin: a critical appraisal of PAH ratios as indicators of PAH source and composition. Org. Geochem. 33, 489–515.
Zhang, G., Li, J., Li, X.D., Xu, Y., Guo, L.L., Tang, J.H., Lee, C.S.L., Liu, X.A., Chen, Y.J., 2010. Impact of anthropogenic emissions and open biomass burning on regional carbonaceous aerosols in South China. Environ. Pollut. 158, 3392–3400.
Zhang, Y.X., Schauer, J.J., Zhang, Y.H., Zeng, L.M., Wei, Y.J., Liu, Y., Shao, M., 2008. Characteristics of particulate carbon emissions from real-world Chinese coal combustion. Environ. Sci. Technol. 42, 5068–5073.